Role of 2C T Cell Receptor Residues in the Binding of Self– and Allo–Major Histocompatibility Complexes

By Peter U.Y. Lee,* Hywyn R.O. Churchill,* Mark Daniels,‡ Stephen C. Jameson,‡ and David M. Kranz*

*From the *Department of Biochemistry, University of Illinois, Urbana, Illinois 61801; and the ‡Department of Laboratory Medicine and Pathology and the Center for Immunology, University of Minnesota Medical School, Minneapolis, Minnesota 55455*

Abstract

T cell clone 2C recognizes the alloantigen L^d and the positive selecting major histocompatibility complex (MHC), K^b. To explore the molecular basis of T cell antigen receptor (TCR) binding to different peptide/MHC (pMHC) complexes, we performed alanine scanning mutagenesis of the 2C TCR. The TCR energy maps for QL9/L^d and SIYR/K^b were remarkably similar, in that 16 of 41 Vα and Vβ alanine mutants showed reduced binding to both ligands. Several TCR residues varied in the magnitude of energy contributed to binding the two ligands, indicating that there are also unique interactions. Residues in complementarity determining region 3α showed the most notable differences in binding energetics among the ligands QL9/L^d, SIYR/K^b, and the clonotypic antibody 1B2. Various lines of evidence suggest that these differences relate to the mobility of this loop and point to the key role of conformational dynamics in pMHC recognition.

Key words: T cell receptor • peptide–major histocompatibility complex • complementarity determining region • alloantigen • antigen recognition

Introduction

Structural analyses of TCR–peptide/MHC (pMHC)[1] complexes have suggested that TCRs interact with pMHC ligands in a conserved, diagonal orientation (1–4). Wiley and colleagues showed that residues at analogous positions on two different TCRs (A6 and B7) contact the same ligand, Tax/HLA-A2, in this conserved orientation (5). In a more recent study, the structure of the A6 TCR was solved in complex with three different peptide variants of Tax, bound to HLA-A2 (6). The complexes appeared to be very similar despite the fact that the peptides have distinct functional effects ranging from antagonist to strong agonist. Thus, there was no obvious correlation between structural features of the complexes and their biological activity (e.g., agonist peptides did not exhibit significant increases in the number of TCR contact residues compared with antagonists).

It is perhaps not surprising that subtle changes in TCR structure dramatically affect function, based on the very narrow energetic windows of TCR–pMHC interactions that underlie different T cell processes (i.e., positive versus negative selection or agonism versus antagonism of mature T cells) (7–9). For example, Gascoigne and colleagues showed that the interaction of a TCR with an agonist and antagonist pMHC exhibited only a threefold difference in affinity (7). Earlier studies revealed that single amino acid differences in a peptide could convert a peptide agonist into an antagonist (10), and it is now widely recognized that the same TCR can be stimulated by a diverse array of peptides (11). The molecular basis for these observations might be best understood in the context of TCR–pMHC binding affinity measurements; the energy derived from a single hydrogen bond could convert an agonist peptide into an antagonist (9).

Although the three-dimensional structures of TCR–pMHC complexes have provided tremendous insight into how a TCR interacts with its ligand, it is not possible from structures alone to understand what constitutes a productive, functional interaction. Discerning the properties of TCR structures that are important in binding and function will require additional approaches. In this regard, the work of Wells has shown that the contact residues identified in three-dimensional structures do not provide a picture of

Address correspondence to David M. Kranz, Department of Biochemistry, University of Illinois, 600 S. Mathews, Urbana, IL 61801. Phone: 217-244-2821; Fax: 217-244-5858; E-mail: d-kranz@uiuc.edu

[1]*Abbreviations used in this paper:* HRP, horseradish peroxidase; pMHC, peptide/MHC complex; SAv, streptavidin; sc, single-chain; wt, wild-type.

 J. Exp. Med. © The Rockefeller University Press • 0022-1007/2000/04/1355/10 $5.00
Volume 191, Number 8, April 17, 2000 1355–1364
http://www.jem.org/cgi/current/full/191/8/1355

the important functional contacts (12). These can only be discerned from a detailed mutagenic study (typically alanine scans) of the protein interface and subsequent binding analyses. Accordingly, it is important to understand which residues of the TCR actually impart the binding energy that is responsible for functional processes and pMHC specificity. One might expect these energy distributions to be similar for the same TCR, binding only minor variants of a single pMHC complex. For example, in the A6–Tax/HLA-A2 system, there are relatively minor differences in total energy and these differences are presumably due to minor alterations at the TCR–pMHC interface. On the other hand, the recognition of self-MHC versus allo-MHC may be considerably different, depending on the structural similarity of the two MHC proteins.

The 2C T cell system (13) provides an opportunity to examine these questions, as multiple pMHC ligands have been identified and it has been thoroughly studied from both structural and functional perspectives. In addition, the 2C TCR has the highest measured affinity for a pMHC ligand, the alloantigen L^d bound to the peptide QL9 (QLSPFPFDL) (14). There are convenient K^b-binding peptides that act as either positive-selecting ligands (EQYKFYSV, called dEV8; 15) or as strong agonists (SIYRYYGL, called SIYR; 16). The structures of unliganded 2C TCR (1) and the 2C TCR–dEV8/K^b (4) complex have been solved, and we recently reported the energy map of the 2C TCR–QL9/L^d interaction (17).

Alanine scanning mutagenesis of TCR–ligand interactions are difficult because of the inherent low affinity of the native TCR (so measurements for alanine mutants with reduced affinities are even more difficult). The 2C TCR–K^b affinities are lower than the 2C TCR–QL9/L^d affinity (K_D = 2 μM for our soluble TCR; 18), making a comparison of energy maps for self-MHC and allo-MHC difficult. In our hands, the affinity of the 2C TCR–dEV8/K^b interaction (K_D > 100 μM) is at least 20-fold lower than the 2C TCR–SIYR/K^b interaction (K_D = 5 μM). In this report, we show that a tetrameric pMHC (SIYRYYGL/K^b) ligand can be used in scans of these low-affinity interactions to construct an energy map of the TCR surface. The approach takes advantage of the avidity of pMHC–streptavidin–horseradish peroxidase (SAv-HRP) tetramers to detect binding multivalent arrays of TCR mutant proteins (19).

A comparison of the 2C TCR energy maps constructed for the allogeneic L^d and the syngeneic K^b showed that most of the same TCR residues were involved in each case. In both cases, CDR1 and CDR2 of the Vα and Vβ contributed the majority of the energy. However, the Vβ appeared to contribute more energy, relative to Vα, in the SIYR/K^b interaction compared with the QL9/L^d interaction. The HV4β also appeared to exert a moderate effect on binding the SIYR/K^b complex. Additional differences in the magnitude of effects were also observed (31αTyr, 55αVal, 28βAsn, and 70βPro affected SIYR/K^b more than QL9/L^d, whereas 29αThr, 49αTyr, and 100αPhe affected QL9/L^d more than SIYR/K^b).

We also analyzed in greater detail the effects of mutations in the CDR3α loop of the 2C TCR, as this loop exhibits the largest conformational difference (6 Å) in unliganded TCR compared with liganded (dEV8/K^b) TCR (4). The results of temperature and mutational analyses support a model in which this loop of the TCR exists in multiple conformations. Stabilization of a conformational state(s) can result in loss of binding to some ligands (QL9/L^d and SIYR/K^b) but strong binding to others (clonotypic antibody 1B2). A solution structure of the D10 TCR showed that the CDR3 loops had considerable mobility (20), consistent with recent thermodynamic studies of two different TCR–pMHC interactions (21). Our findings suggest that there are severe functional consequences to restricting this mobility.

Materials and Methods

TCR Expression and Purification. The 2C TCR was expressed in *Escherichia coli* as a single-chain (sc) protein as described previously (17, 22). Wild-type (wt) and single-site mutant scTCR were refolded from inclusion bodies and purified over a denaturing nickel affinity column. Monomeric scTCR was isolated by HPLC G-200 size exclusion chromatography, and the purity of the monomeric protein was assessed by SDS-PAGE.

mAbs. F23.1 is a mouse IgG2a mAb specific for Vβ8.1, Vβ8.2, and Vβ8.3 (23). 1B2 is a clonotypic mAb specific for the Vα and Vβ of the 2C TCR (24). Both antibodies were purified from ascites by ammonium sulfate precipitation followed by DEAE-cellulose chromatography. 1B2 binding to scTCR was examined in a capture ELISA in which F23.1 mAb was immobilized on Immulon plates (Dynatech Technologies). Wells were washed with 0.5% BSA and 0.05% Tween 20 in PBS, and then 50 μl of wt or mutant scTCR was added at 10 μg/ml. After 30 min at 4°C, wells were washed and biotin-labeled 1B2 mAb was added at various dilutions. Binding was detected with the addition of SAv-HRP and tetramethylbenzidine (TMB)-peroxidase substrate (Kirkegaard & Perry).

Preparation of SIYR/K^b Tetramers. Biotinylated SIYR/K^b was prepared by labeling the refolded complex at a BirA recognition sequence located at the COOH terminus of the MHC α chain using the BirA enzyme (Avidity). Monomeric biotinylated SIYR/K^b was isolated by HPLC G-200 size exclusion chromatography. Tetramers were prepared by incubating the biotinylated SIYR/K^b complexes with SAv-HRP at a calculated molar ratio of >200:1 biotinylated pMHC to SAv-HRP by addition of biotinylated SIYR/K^b to SAv-HRP over 6 h at 4°C. In preliminary experiments, preparations of 4:1 and 200:1 SIYR/K^b–SAv-HRP were compared for their binding to wt TCR and two mutants (αY49A and αF100A). Although the relative binding values for each preparation were completely consistent among the three different TCR proteins, the 200:1 preparation had a considerably higher signal and accordingly was used for analyses of all mutants. Two different commercial preparations of SAv-HRP (Kirkegaard & Perry) were also examined at the 200:1 ratio and were found to have significant differences in their activity. It is possible that these differences relate to the SAv-HRP heterogenity derived from chemical coupling of HRP (e.g., some SAv molecules are likely to be unlabeled with HRP and might compete with labeled molecules, and some SAv molecules are likely to be labeled at the biotin binding sites and therefore would exhibit lower valencies).

Peptide–MHC Binding Assays. Direct adsorption of scTCR to

wells did not yield detectable binding by either SIYR/K^b tetramers or 1B2, probably because the scTCR was immobilized in an orientation that was not accessible to these ligands. Because the F23.1 epitope does not overlap with the binding sites for either SIYR/K^b or 1B2, we used adsorbed F23.1 mAb as a way to orient the scTCR in a uniform multivalent layer. 50 μl of F23.1 mAb (10 μg/ml) was adsorbed to Immulon wells, which were then washed, and scTCR preparations were added. In initial experiments, the concentration of scTCR (wt or mutant) was varied to explore the sensitivity of the assay. All subsequent experiments that involved titrations of SIYR/K^b tetramers involved the use of scTCR at a saturating concentration of 10 μg/ml. After incubation with scTCR, wells were washed and then incubated with 50 μl of a dilution of SIYR/K^b tetramer or 1B2 for 30 min. After washing, binding was detected by addition of TMB-peroxidase substrate. Except where noted, binding assays of scTCR mutants were performed at 4°C because this is the temperature at which the alanine scan of the 2C–QL9/L^d interaction was performed (17). The relative reactivities of wt TCR and mutants αY49A and αF100A incubated with SIYR/K^b at two different temperatures (4°C and 25°C) and for various times (30, 60, and 120 min) were completely consistent.

The wt scTCR and several mutants (βT55A, βQ72A, αY49A, and αF100A) were also examined by a similar F23.1 capture ELISA, titrated at various concentrations of QL9/L^d Ig dimer (25, 26). Bound QL9/L^d Ig dimer was detected with HRP-labeled goat anti–mouse λ (Southern Biotechnology Associates).

Analysis of Binding Data. Binding data from the pMHC tetramer ELISAs were initially analyzed by three different parameters to determine the most reliable measure of activity: maximum absorbance achieved at the highest concentration of ligand (tetramer or 1B2), concentration of ligand at half-maximal binding, and slopes of regression lines from double reciprocal plots ((absorbance^{-1}) versus $(\text{tetramer concentration}^{-1})$). Although all three parameters yielded the same relative activities for the wt scTCR and the array of alanine mutants, the slopes from double reciprocal plots were found to be least subject to variability from assay to assay. Thus, these slopes were used to establish the relative reactivities, calculated as the logarithm of (the slope of mutant scTCR divided by the slope of wt scTCR). Those mutants that did not exhibit detectable binding to the tetramer complex were considered to have >15-fold reduced binding, which was the approximate working range of relative reactivities. This limit was also approximately that found with a different pMHC binding assay in the alanine scan of the 2C–QL9/L^d interaction (17).

Structural Analysis. The crystal structure of the 2C–dEV8/K^b complex (4) was used as a guide to interpret the alanine scan of the 2C–SIYR/K^b interaction. The QUANTA software package (Molecular Simulations) was used on a Silicon Graphics O_2 workstation. Peptide versus MHC reactivity assignments were made based on the structure of the 2C–dEV8/K^b complex. QUANTA was also used to display the conformations of the CDR3α region in its liganded (2C–dEV8/K^b) and unliganded (2C TCR) forms.

Results and Discussion

Binding of 2C TCR to SIYR/K^b Tetramers. Previous work with soluble versions of the 2C TCR showed that an scTCR with an NH_2-terminal thioredoxin fusion increased its solubility such that it could be used to monitor binding to the QL9/L^d alloantigen (22). Thus, a panel of alanine mutants of the 2C scTCR were used to determine, in a quantitative competition assay with ^{125}I-labeled anti-L^d Fab fragments, the binding energy associated with each mutant protein (17). Similar assays to examine the binding of the scTCR to the agonist peptide SIYR bound to the positive selecting class I molecule K^b were unsuccessful (data not shown), most likely because of the lower affinity of the 2C TCR–SIYR/K^b interaction. Recent studies have shown that cell surface binding of soluble pMHC to the TCR can be detected by increasing the avidity of the interaction through the use of pMHC tetramers (19). This suggested to us that a similar approach might allow the detection of recombinant TCR, if the TCR were arrayed in a multivalent layer in an ELISA format.

Soluble, refolded scTCRs were added to wells that contained the anti-Vβ antibody F23.1 (23). F23.1 recognizes a framework region of the Vβ8 domain, and its binding site does not overlap with that of either pMHC or the clonotypic antibody 1B2 (17). After addition of scTCR, wells were washed and incubated with a tetramer of biotinylated SIYR/K^b bound to SAv-HRP, followed by substrate. Each scTCR was assayed at various concentrations of the tetramer to construct titration curves of the wt 2C scTCR and the panel of alanine mutants (Fig. 1). No binding was detected in the absence of the TCR or the biotinylated K^b, and the binding of the tetrameric SIYR/K^b could be completely blocked with the anticlonotypic antibody 1B2, which recognizes an epitope that is very similar to the pMHC binding site (data not shown). Because this binding assay involves multivalent interactions, it was not possible

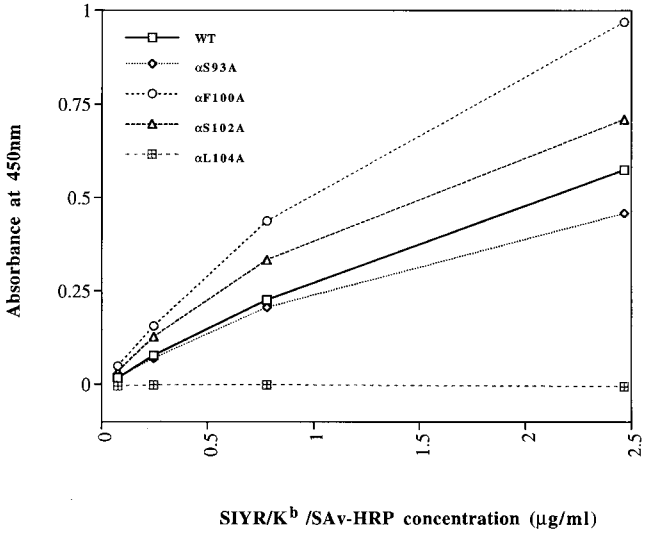

Figure 1. SIYR/K^b tetramer complexes binding to wt 2C scTCR and to representative scTCR alanine mutants. SIYR/K^b tetramer binding was examined in a capture ELISA. scTCR was added to immobilized F23.1 mAb, and then various concentrations of the SIYR/K^b–SAv-HRP tetramer were added, followed by incubation with substrate. Binding was completely inhibited by unlabeled clonotypic 1B2 antibody (data not shown), indicating that the pMHC binds at the expected TCR binding site.

to calculate the intrinsic binding constant for each scTCR mutant. Various strategies were explored to determine the most appropriate parameter for comparing wt scTCR binding to the mutant scTCR (see Materials and Methods). Ultimately, the slope of double reciprocal plots (absorbance^{-1} versus concentration^{-1}) were found to be reliable measures of binding, and calculations of binding contribution were made relative to wt scTCR. The range of values (log reactivity relative to wt scTCR) for the entire panel of 46 mutants was found to be very similar to the actual range of energies ($\Delta\Delta G$) calculated in the QL9/L^d binding study (see below and reference 17).

Effect of Alanine Mutations on SIYR/K^b Binding. Tetramer (SIYR/K^b–SAv-HRP) titrations of the 46 different single-site mutants within the CDR and HV loops of the 2C TCR were performed (Fig. 2). The majority of residues that influenced binding most significantly were in CDR1 and CDR2 of the Vα and Vβ. This finding is consistent with the distribution of contact residues in the structure of the 2C TCR–dEV8/K^b complex (4). Although none of the HV4α residues appeared to affect SIYR/K^b recognition, several HV4β region residues (70βPro, 72βGln, and 76βSer) had moderate effects. These results could be due to direct interactions with pMHC or through indirect effects on other CDR loops. For instance, the HV4β is in close proximity to CDR1β and CDR2β, which have significant effects on SIYR/K^b binding and 72βGln hydrogen bonds with the main-chain oxygen of 28βAsn. On the other hand, the differences between the effects of HV4β mutations on SIYR/K^b compared with QL9/L^d binding (see below) may suggest additional direct interactions with SIYR/K^b.

The following residues contact either peptide dEV8 or K^b in the structure and, based on a reduction in binding of the alanine mutant (more than threefold compared with wt), contribute significant energy to binding: 26αTyr (K^b), 31αTyr (peptide/K^b), 50αTyr (K^b), 28βAsn (K^b), 31βAsn (peptide), 50βTyr (K^b), and 97βGly (peptide/K^b). As in other alanine scans, some residues shown to be in contact in the crystal structure do not appear to contribute energy to the interaction. The following residues contact either dEV8 or K^b in the structure but did not contribute significant energy to binding: 27αSer (K^b), 51αSer (K^b), 93αSer (peptide), 100αPhe (peptide/K^b), 26βThr (K^b), 55βThr (K^b), and 56βGlu (K^b). Finally, some residues within the CDR and HV loops do not contact either dEV8 or K^b in the structure but the alanine mutants exhibited a significant reduction in binding: 30αPro, 49αTyr, 55αVal, 104αLeu, 27βAsn, 30βAsn, 48βTyr, 70βPro, and 106βLeu. It has been thought that mutations such as these could act through destabilization of adjacent residues or loops, as most of them are in close proximity to other residues. However, evidence suggests that some mutations may stabilize the TCR, which could also lead to reduced binding (e.g., 104αLeu; see CDR3α below). In these latter cases, there may be a reduction in entropy associated with decreased conformational mobility, and this mobility may be necessary for binding of some ligands.

There has been particular interest in the role of Vα residues 27 and 51 in pMHC binding (27). These residues

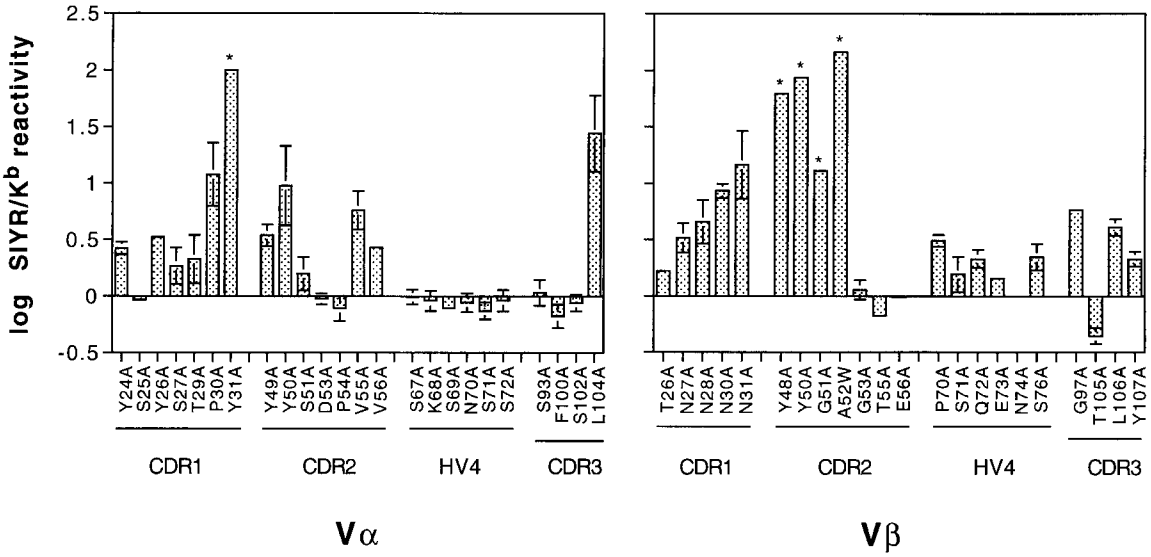

Figure 2. Binding of SIYR/K^b to single-site 2C scTCR mutants. The relative reactivity of SIYR/K^b binding to scTCR mutants was calculated from double reciprocal plots (absorbance^{-1} versus tetramer concentration^{-1}) of the binding data shown in Fig. 1, as described in Materials and Methods. Bars that extend above the zero line indicate mutants that exhibit decreased binding to SIYR/K^b compared with wt scTCR. Bars that extend below the zero line indicate mutants that show improvement in binding to SIYR/K^b. Error bars indicate the SD calculated from two or more experiments. Mutant scTCR indicated by an asterisk (*) exhibited significantly reduced but detectable binding in one assay (actual values shown) but no detectable binding in other assays. Mutant αY31A did not show binding to SIYR/K^b in any assay and was considered to be below the limit of detection in this assay (approximated in the value shown).

have been implicated in the CD4/CD8 skewing associated with the Vα3 system (28), and they are in direct contact with K^b residues (Glu 58 and Arg 62 of K^b contacting TCR 27αSer, and Ala 152, Gly 162, and Glu 166 of K^b contacting TCR 51αSer). As recently observed for the QL9/L^d interaction (18), alanine mutations at TCR positions Serα27 and Serα51 had little effect on SIYR/K^b binding (Fig. 3). It is possible that there is a compensatory involvement of water molecule(s) in the alanine mutants or that these residues impact T cell function through effects on kinetics rather than equilibrium binding, as we have recently suggested (18). Because polymorphisms at these positions (Pheα27 and Proα51) have been shown to skew $V\alpha3^+$ T cells to the CD8 phenotype in an H-2^b background, we also examined the effects of these mutations, individually and together, on SIYR/K^b binding. The original expectation was that the Pheα27 and Proα51 residues may act by increasing the affinity of the TCR for class I, thereby skewing selection of the T cell into the CD8 compartment. However, as observed for QL9/L^d binding, these mutations had negative effects on binding of the 2C TCR to SIYR/K^b (Fig. 3). This result is consistent with the quantitative instruction model of lineage commitment (29, 30), which predicts that higher affinity TCR interactions (27αSer and 51αSer) skew cells toward a CD4 lineage or deletion, whereas moderate affinity TCR interactions skew cells toward a CD8 lineage (27αPhe and 51αPro). It is also possible that at least some T cells do not require the TCR–class II interaction at all to complete development along the CD4 lineage (31).

Comparison of TCR Energy Maps for Binding to SIYR/K^b and QL9/L^d. An alanine scan does not address the role of interactions between the peptide backbone of the TCR and pMHC. Although these interactions contribute energy to the overall interaction and may in some cases be pMHC specific, they cannot be responsible for the diversity and specificity associated with pMHC recognition. The fact that the 2C TCR recognizes two very different pMHC complexes allows us to examine if the TCR residues responsible for these specificities differ. Binding data for the 2C TCR mutants with self-MHC (this report) and allo-MHC ligands (17) were used to construct TCR energy maps for both interactions. Fig. 4 compares the hot spots of binding associated with 2C TCR binding to SIYR/K^b and QL9/L^d. Both interactions involve two hot spots that lie diagonally over the MHC helices. Overall, the same regions of the TCR at the interface are involved in binding each ligand, with subtle but significant changes in the role of individual residues. These appear to be largely differences in the magnitude of the contribution rather than the presence or absence of an effect. The most significant differences were residues 31αTyr, 55αVal, 28βAsn, 70βPro, and 72βGln, which affected SIYR/K^b more than QL9/L^d, and 29αThr, 49αTyr, and 100αPhe, which affected QL9/L^d more than SIYR/K^b. Several mutants were examined with QL9/L^d Ig dimer to confirm that these differences were not a consequence of reduced mobility or increased valency with the SIYR/K^b–SAv-HRP approach. The results with the QL9/L^d Ig dimer were completely identical to those obtained with monomeric QL9/L^d in the previously reported alanine scan (i.e., binding order: βT55A > wt > βQ72A > αF100A > αY49A; data not shown and reference 17).

Thus, the overall TCR energy distribution appears to have been shifted slightly from the peptide NH_2 end in QL9/L^d binding to the peptide COOH end in SIYR/K^b. A recent study showed that two mAbs specific for the OVA-8/K^b complex mapped to the peptide COOH end of the complex (32). One interpretation of these results is that this region of the K^b molecule is more accessible than L^d.

Table I summarizes the approximate relative binding energies contributed by each of the 2C TCR loops. As suggested from the representation shown in Fig. 4, there is remarkable similarity in the role of TCR regions for binding both the self- and the allo-MHC ligands. These similarities may derive from the overall surface topology of the pMHC complex (i.e., only particular regions are exposed and thus potential contact areas). Furthermore, selection on a class I MHC during thymic development (K^b in this case) predisposes TCR residues to be involved in structurally related allo-MHC molecules (L^d in this case). However, it is also of interest that there appears to be an increase in binding energy associated with the Vβ chain and SIYR/K^b recognition compared with QL9/L^d recognition. The increased Vβ involvement is due largely to the HV4 loop, suggesting that this may play a greater role in SIYR/K^b contact than in QL9/L^d contact. Speir et al. have suggested that the HV4 region (69βArg in particular) could contribute electrostatic forces to the interaction with ligand, but their model suggested that this effect would be more pro-

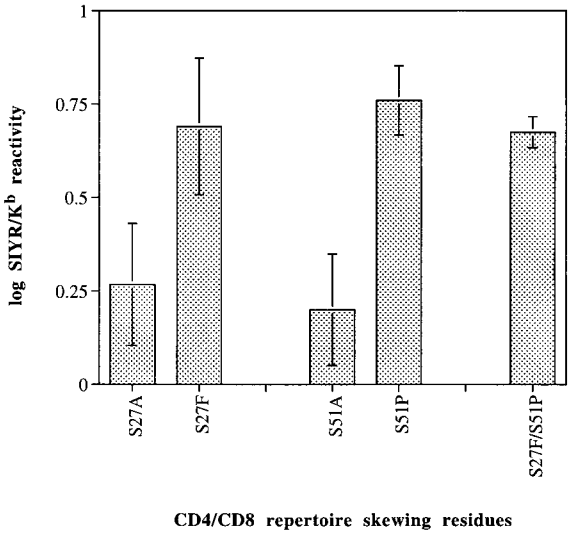

Figure 3. Binding of SIYR/K^b to scTCR mutants known to be involved in CD4/CD8 repertoire skewing. The reactivity of alanine mutants (S27A and S51A) as well as CD8 skewing mutants (S27F, S51P, and double mutant S27F/S51P) was calculated relative to wt scTCR as described in the legend to Fig. 2 and in Materials and Methods. Error bars indicate the SD calculated from two or more assays.

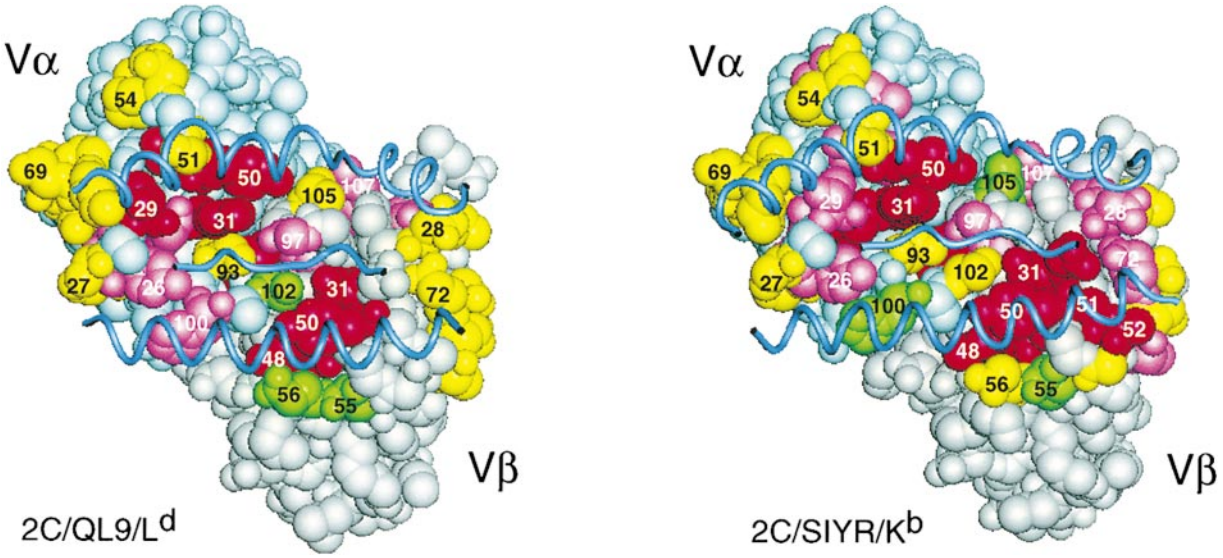

Figure 4. Energy maps of the 2C TCR binding sites for QL9/L^d and SIYR/K^b. CDR and HV4 region residues are highlighted based on their influence on peptide–MHC binding, when mutated to alanine. Red indicates those residues with the greatest effect on binding; pink are those residues with an intermediate effect; yellow are those residues with a negligible effect; and green are those residues that exhibit improved binding. The 2C–QL9/L^d epitope, previously determined by Manning et al. (reference 17), is shown with the QL9/L^d MHC helices and peptide superimposed. The 2C–SIYR/K^b epitope, determined in this study, is shown with the dEV8/K^b MHC helices and peptide superimposed. The refined crystal structure of the 2C–dEV8/K^b complex was used to establish the orientation of pMHC binding to TCR. Several alanine mutants (αV56A, βN30A, βG51A, βA52W, and βG53A) were not tested for QL9/L^d binding but are included in the dEV8/K^b map.

nounced in the 2C TCR–QL9/L^d interaction (33). A structure of the 2C TCR–QL9/L^d complex would be necessary to determine if the 2C Vβ is positioned differently than in the SIYR/K^b complex. There is precedence for reduced involvement of a Vβ chain in the A6–Tax/HLA-A2 structure (2).

Table I. *Percent Contributions of CD4 and HV4 Regions to Binding SIYR/K^b and QL9/L^d*

	SIYR/K^b	QL9/L^d
CDR1α	26	33
CDR2α	17	17
HV4α	−3	2
CDR3α	7	10
CDR1β	18	15
CDR2β	15	14
HD4β	11	0
CDR3β	9	9
Vα	47	62
Vβ	53	38

The percentage of total energy distributed among the different CDR and HV regions was calculated from log reactivity values (SIYR/K^b) or free energy (ΔΔG) values (QL9/L^d from reference 17). To standardize the comparison, maximum reductions in binding for each assay were set at 15-fold (because of the slightly different sensitivities of the two assay formats). Residues that were not tested for QL9/L^d binding (see text) were not included in the SIYR/K^b calculations.

It is interesting that the distribution of energetic contacts displays a twofold symmetry of binding across the diagonal axis. In fact, residues at the equivalent positions in the Vα and Vβ (positions 31 and 50) appear to be the key focal points of binding, perhaps analogous to homodimers that form in other receptor–ligand interactions. Although this dimeric configuration cannot be generally true of all TCRs (based on the observation that at least the A6–Tax/HLA-A2 interaction does not involve Vβ CDR1 and CDR2 [2]), it is possible that different Vα and Vβ have evolved residues at these positions to facilitate binding along this twofold axis of symmetry. This could account in part for earlier observations that some Vβ regions were predisposed to interact with particular MHC alleles (34) and that there appears to be preferential expression of specific VαVβ pairs (35, 36).

The distribution of energy among TCR side chains that contact peptide or MHC is approximately the same in the TCR–SIYR/K^b and TCR–QL9/L^d interactions. Thus, about one third of the energy is directed at the peptide and two thirds of the energy is directed at the helices. Such bias towards the MHC helices in the interaction with syngeneic MHC could account for findings that unrelated peptides can activate mature T cells (37) and that many peptides can participate in the positive selection process (38). As discussed previously, interactions with MHC helices selected during thymic development can provide a basal affinity, whereas interactions with peptide provide sufficient increases in energy to drive T cell activity and confer peptide specificity (9).

TCR Energy Map for Binding to SIYR/K^b and Epitope Map of Key K^b Residues. A study by Nathenson and colleagues several years ago used a panel of K^b mutants and various K^b-restricted and alloreactive T cell clones to identify the regions of the K^b helices that are involved in T cell recognition (39). The results suggested that two regions at opposite positions on the two helices contain hot spots for TCR recognition, leading to the first proposal that the TCR may orient diagonally on the pMHC. Superimposing the K^b helices, with the eight key residues highlighted, on the 2C TCR energy map shows that these K^b residues reside very near the TCR hot spots identified in our alanine scan (Fig. 5). Six of the K^b residues were located within 3.8–10.7 Å of a TCR residue determined to contribute significant energy to the interaction. The two most distal residues (Leu82 and Asn174) were located 12 and 15 Å from the nearest TCR residue found to be important in binding. Interestingly, all 8 of these K^b residues are identical in the L^d molecule, even though K^b and L^d differ by a total of 41 residues (14 in α1, 18 in α2, and 9 in α3). Thus, we predict that in alloreactivity the majority of the TCR binding energy is focused on those residues that are shared between the self-MHC restricting element and the allo-MHC, and that the additional energy derived from minor differences in MHC and/or peptide are sufficient to elicit agonist activity.

As discussed above, some of the interactions involving these K^b residues involve TCR backbone contacts that would not be assessed in an alanine scan. As 30–90% of the 59 T cell clones in the Sun et al. study were affected by the set of K^b mutations highlighted in Fig. 5 (39), it is reasonable to predict that other TCRs will exhibit energy distributions similar to the 2C TCR. Conversely, do other class I MHC alleles have similar hot spots that are recognized by different TCRs? The observation that the 2C TCR energy map is nearly identical whether the MHC ligand is K^b or L^d supports this possibility. Additional evidence has come from several observations: (a) limited mutagenesis of other class I molecules, including a recent study of L^d (40), is consistent with the general contact areas shown in Fig. 5; (b) many alloreactive T cell clones raised in K^b-negative mice (and therefore with quite different positive-selecting class I molecules) still recognized this same pattern on the K^b molecule (39); and (c) the crystal structures of TCR–pMHC complexes have so far uniformly illustrated the conserved topology of these interactions. The supposition that TCRs have evolved to recognize MHC (41) suggests that the critical residues found within the hot spot regions of the TCR represent the target of such longer term selection.

Effect of CDR3α Mutations: Evidence of Multiple Conformational States of the TCR. The CDR3 loop of the 2C TCR (SGFASAL) exhibits the largest difference in structure when comparing the unliganded 2C TCR and the liganded TCR (TCR–dEV8/K^b) (4). In the liganded structure the apical residue, Phe100, has moved 6 Å such that it is aligned along the axis of the K^b α1 helices (Fig. 6). This movement appears to be necessary to allow the TCR to dock onto the pMHC without interference from the protruding side chain of Phe100. Comparison of the effects of the CDR3α alanine mutants on the three ligands (Fig. 7 A) revealed significant differences that are in part related to the conformational flexibility of this loop. The F100A mutant

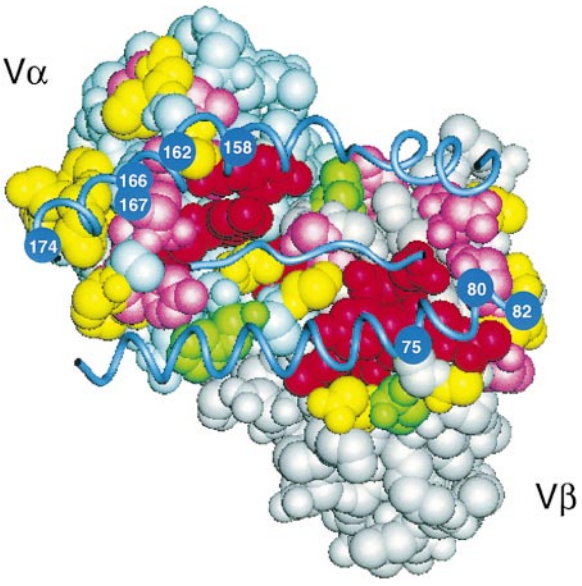

Figure 5. Location of K^b residues known to affect activity of K^b-restricted or alloreactive T cell clones. H-2K^b residues that were previously identified as important in the activity of a panel of 59 T cell clones (reference 39) are superimposed on the 2C–SIYR/K^b epitope. Single-site mutations at the eight highlighted K^b residues (blue circles) were shown to affect T cell activity of 30–90% of the T cell clones tested (reference 39). Six of the K^b residues are in close proximity to TCR residues that influenced binding of peptide–MHC, whereas two residues (Leu82 and Asn174) are >10 Å from the nearest TCR residue (pink or red) that had a significant effect on SIYR/K^b binding. All eight residues are identical in L^d.

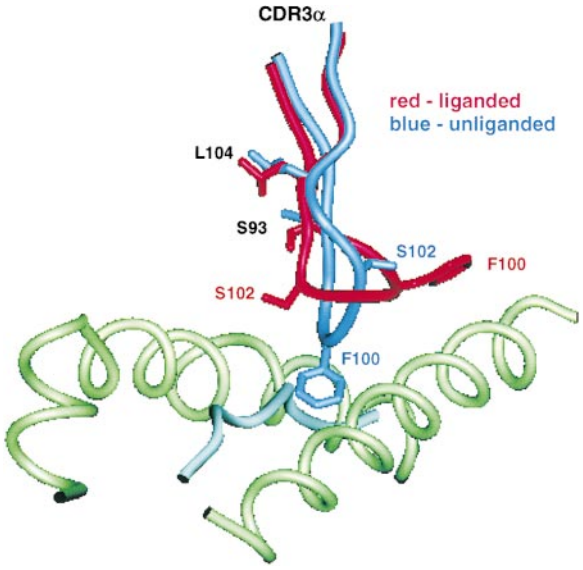

Figure 6. 2C CDR3α loop in liganded and unliganded conformations. CDR3α in its unliganded state (blue strand) is superimposed on the structure of CDR3α in its bound state with dEV8/K^b pMHC (red strand) generated from crystal structures of the unliganded 2C TCR (reference 1) and the 2C–dEV8/K^b complex (reference 4).

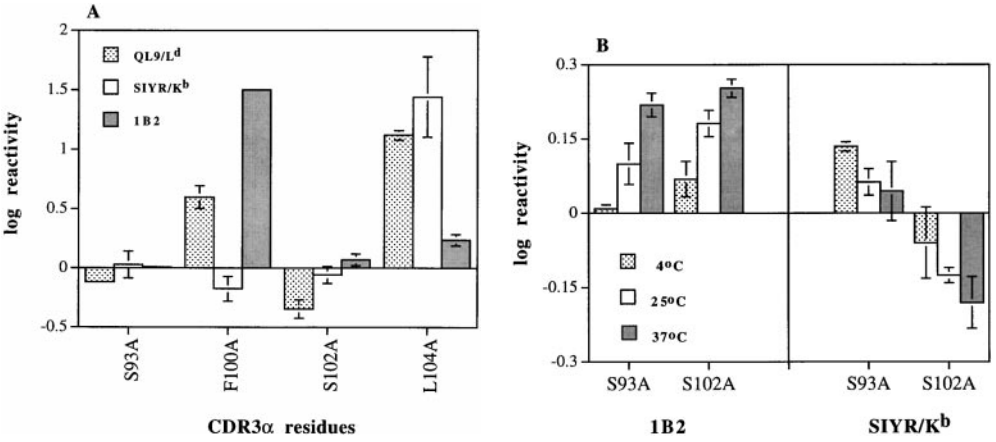

Figure 7. Effect of CDR3α mutations on binding to QL9/L^d, SIYR/K^b, and mAb 1B2. (A) Effect of 2C TCR CDR3α mutations on binding the three different ligands at 4°C. Reactivity of CDR3α alanine mutants for SIYR/K^b tetramer complexes and mAb 1B2 was assessed in ELISAs as described in Materials and Methods. QL9/L^d reactivity was determined in a competition assay with ^{125}I-labeled anti-L^d Fab fragments as reported previously (reference 17). (B) Effect of temperature on mAb 1B2 and SIYR/K^b binding to Vα mutants S93 and S102. Binding of scTCR alanine mutants S93 and S102 was tested at 4°C, 25°C, and 37°C. Error bars indicate the reactivity values calculated from two independent ELISA titrations.

of the 2C TCR showed the greatest variation in binding effects, of all of the TCR residues, to the three ligands 1B2, QL9/L^d, and SIYR/K^b. Phe100 was the most important residue for binding 1B2, it had a moderate contribution to QL9/L^d binding, and it had, if anything, a negative effect on binding to SIYR/K^b. Based on the structures of this TCR, these results are consistent with the possibility that there is an entropic penalty in binding the K^b ligand. We propose that in the TCR–1B2 complex, Phe100 is a contact residue that is associated directly with 1B2 CDRs, perhaps in a conformation that is close to that of the unliganded TCR (accordingly, there would not be a loss of binding energy due to entropic effects). The intermediate effect of binding to the QL9/L^d ligand leads to the prediction that the Phe100 may be in yet a different conformation in the QL9/L^d complex.

L104A of CDR3α was the only alanine mutant tested that had a significant effect on binding of the pMHC complexes but no effect on the binding of 1B2. As shown in Fig. 6, Leu104 is not positioned near the binding site but is buried and in proximity to residues from other CDRs. Thus, the considerable reduction in binding of pMHC is likely to be due to effects of the alanine substitution on the conformation of this region of the receptor. How might this alanine mutation exert such effects? Evidence suggests that this mutation may act by altering the conformational states of the CDR3α loop. We have recently shown that a proline mutation at this position (L104P) increases the thermal stability of the TCR, yet this mutant has the same binding properties as the L104A mutant (i.e., it binds 1B2 but does not bind QL9/L^d) (42, 43). This finding is consistent with the possibility that the CDR3α loop is stabilized in the L104 mutants in the "unliganded" conformation, capable of binding 1B2 but not pMHC. This proposed mechanism is in accord with the observation that CDR3α exhibits the largest conformation difference in bound and unbound states.

Recent studies showed that temperature had unexpected effects on TCR–pMHC binding, suggesting that there is flexibility in the TCR (21) or perhaps even conformational changes that lead to TCR dimerization (44). We have also found that some 2C TCR–pMHC interactions may increase their binding affinities with an increase in temperature, consistent with a large entropic contribution that might be associated with conformational flexibility (45). To explore this further, we examined the effects of temperature on binding by alanine mutants of the two residues in CDR3α (Ser93 and Ser102) that had minimal effect on binding to either 1B2 or pMHC (Fig. 7 A). Each of these mutants was titrated at 4°C, 25°C, and 37°C with the ligands 1B2 and SIYR/K^b, and binding activity was calculated relative to the wt TCR (Fig. 7 B). The binding of 1B2 and SIYR/K^b showed completely opposite effects for both mutants: an increase in temperature led to reduced binding for 1B2, whereas an increase in temperature led to increased binding for SIYR/K^b. Although it is not possible to calculate enthalpy values directly from this assay, the effects are consistent with an unfavorable entropic contribution associated with the presence of serine residues at these positions. Accordingly, alanine substitutions at these positions could affect the flexibility of the loop (albeit to a lesser degree than the Leu104 mutations). In this model, binding of SIYR/K^b benefits from the increased CDR3α movement at higher temperatures because this ligand requires that the TCR bind in a conformation that represents a low frequency state of the TCR. In contrast, 1B2 binding is reduced at higher temperatures because this ligand interacts with the predominant, unliganded conformation of the TCR, and at higher temperatures this state is less frequent.

The binding of the anticlonotypic antibody 1B2 to the predominant TCR conformation might be expected from the manner in which this antibody was generated. 1B2 is a high affinity antibody that was isolated from a mouse that

had been immunized six times with native clone 2C T cells (13). Clonotypic antibodies are notoriously difficult to produce and thus those that are identified are likely to recognize the TCR conformation that predominates in the immunogen preparation. In contrast, there appears to be less selective pressure for high affinity interactions of the TCR with pMHC, and in fact such interactions would normally lead to T cell deletion during thymic development.

Although the crystal structures of the 2C TCR represent two possible conformations of the TCR, there are very likely dynamic and heterogeneous forms in the unliganded, solution state. In fact, a recent solution structure of the D10 TCR has shown that CDR3 loops exhibited the greatest mobility among the regions of the scTCR that were analyzed (20). As they suggest, hydrogen bonding (as seen for several of the serine residues in the 2C TCR crystal structure) may restrict mobility and thereby affect the entropy of the interactions. Such effects may in part account for our observations that serine residues of the 2C TCR frequently exhibit no effect when changed to alanine or even display increases in affinity (18). The observations that on-rates of TCR–pMHC interactions are typically slower than the on-rates of antibody–antigen interactions (8, 46) are consistent with the notion that most TCRs are in dynamic equilibrium among various conformations and that the lower frequency forms bind to the pMHC ligands. Similar observations have been made for antibodies, especially those of low affinity that have been isolated after a single immunization (47). A germline-encoded antibody showed different conformations in the free and bound states, whereas the unbound form of a high affinity variant adopted a conformation similar to that of the germline antibody in the bound state (48). A recent study provided both kinetic and thermodynamic evidence that TCR–pMHC binding exhibited an unfavorable entropic component, suggesting that a particular TCR conformation is stabilized in the bound state (21). Consequently, a proposed induced-fit mechanism suggests that TCRs scan multiple pMHC complexes until a particular structural interaction gives rise to folding transitions that allow TCR binding (49). The presence of many conformations within a single TCR could provide the T cell an opportunity to recognize many different peptide–MHC molecules (11, 50), either because it is advantageous to do so during positive selection or because this increases the functional diversity already generated in the TCR repertoire through genetic mechanisms.

We wish to thank Thomas Manning, Carol Schlueter, and Thomas Brodnicki for producing most of the single-site mutants used in this study, Sean O'Herrin for providing QL9/L^d Ig dimers, and Ian Wilson for discussions regarding the 2C TCR crystal structures. We also wish to acknowledge services provided by the Genetic Engineering Facilities at the University of Illinois.

This work was supported by National Institutes of Health grant GM55767 (to D.M. Kranz).

Submitted: 19 November 1999
Revised: 25 January 2000
Accepted: 10 February 2000

References

1. Garcia, K.C., M. Degano, R.L. Stanfield, A. Brunmark, M.R. Jackson, P.A. Peterson, L. Teyton, and I.A. Wilson. 1996. An αβ T cell receptor structure at 2.5 angstrom and its orientation in the TCR-MHC complex. *Science*. 274:209–219.
2. Garboczi, D.N., P. Ghosh, U. Utz, Q.R. Fan, W.E. Biddison, and D.C. Wiley. 1996. Structure of the complex between human T-cell receptor, viral peptide and HLA-A2. *Nature*. 384:131–141.
3. Teng, M.K., A. Smolyar, A.G. Tse, J.H. Liu, J. Liu, R.E. Hussey, S.G. Nathenson, H.C. Chang, E.L. Reinherz, and J.H. Wang. 1998. Identification of a common docking topology with substantial variation among different TCR-peptide-MHC complexes. *Curr. Biol.* 8:409–412.
4. Garcia, K.C., M. Degano, L.R. Pease, M. Huang, P. Peterson, L. Teyton, and I.A. Wilson. 1998. Structural basis of plasticity in T cell receptor recognition of a self peptide-MHC antigen. *Science*. 279:1166–1172.
5. Ding, Y.H., K.J. Smith, D.N. Garboczi, U. Utz, W.E. Biddison, and D.C. Wiley. 1998. Two different T cell receptors bind in a similar diagonal mode to the HLA-A2/Tax peptide complex using different TCR amino acids. *Immunity*. 8:403–411.
6. Ding, Y.H., B.M. Baker, D.N. Garboczi, W.E. Biddison, and D.C. Wiley. 1999. Four A6-TCR/peptide/HLA-A2 structures that generate very different T cell signals are nearly identical. *Immunity*. 11:45–56.
7. Alam, S.M., P.J. Travers, J.L. Wung, W. Nasholds, S. Redpath, S.C. Jameson, and R.J. Gascoigne. 1996. T cell receptor affinity and thymocyte positive selection. *Nature*. 381:616–620.
8. Davis, M.M., J.J. Boniface, Z. Reich, D. Lyons, J. Hampl, B. Arden, and Y. Chien. 1998. Ligand recognition by alpha beta T cell receptors. *Annu. Rev. Immunol.* 16:523–544.
9. Manning, T.C., and D.M. Kranz. 1999. Binding energetics of T-cell receptors: correlation with immunological consequences. *Immunol. Today*. 20:417–422.
10. Sloan-Lancaster, J., and P.M. Allen. 1996. Altered peptide ligand-induced partial T cell activation: molecular mechanisms and role in T cell biology. *Annu. Rev. Immunol.* 14:1–27.
11. Mason, D. 1998. A very high level of crossreactivity is an essential feature of the T-cell receptor. *Immunol. Today*. 19: 395–404.
12. Wells, J. 1991. Systematic mutational analyses of protein-protein interfaces. *Methods Enzymol.* 202:390–411.
13. Kranz, D.M., D.H. Sherman, M.V. Sitkovsky, M.S. Pasternack, and H.N. Eisen. 1984. Immunoprecipitation of cell surface structure of cloned cytotoxic T lymphocytes by clone-specific antisera. *Proc. Natl. Acad. Sci. USA*. 81:573–577.
14. Sykulev, Y., A. Brunmark, T.J. Tsomides, S. Kageyama, M. Jackson, P.A. Peterson, and H.N. Eisen. 1994. High-affinity reactions between antigen-specific T-cell receptors and peptides associated with allogeneic and syngeneic major histocompatibility complex class I proteins. *Proc. Natl. Acad. Sci. USA*. 91:11487–11491.
15. Tallquist, M.D., T.J. Yun, and L.R. Pease. 1996. A single T cell receptor recognizes structurally distinct MHC/peptide complexes with high specificity. *J. Exp. Med.* 184:1017–1026.
16. Udaka, K., K. Wiesmuller, S. Kienle, G. Jung, and P. Walden. 1996. Self-MHC-restricted peptides recognized by an alloreactive T-lymphocyte clone. *J. Immunol.* 157:670–678.
17. Manning, T.C., C.J. Schlueter, T.C. Brodnicki, E.A. Parke, J.A. Speir, K.C. Garcia, L. Teyton, I.A. Wilson, and D.M. Kranz. 1998. Alanine scanning mutagenesis of an αβ T cell receptor: mapping the energy of antigen recognition. *Immu-*

nity. 8:413–425.
18. Manning, T.C., E.A. Parke, L. Teyton, and D.M. Kranz. 1999. Effects of complementarity determining region mutations on the affinity of an αβ T cell receptor: measuring the energy associated with CD4/CD8 repertoire skewing. *J. Exp. Med.* 189:461–470.
19. Altman, J.D., P.A.H. Moss, P.J.R. Goulder, D.H. Barouch, M.G. McHeyzer-Williams, J.I. Bell, A.J. McMicheal, and M.M. Davis. 1996. Phenotypic analysis of antigen-specific T lymphocytes. *Science.* 274:94–96.
20. Hare, B.J., D.F. Wyss, M.S. Osburne, P.S. Kern, E.L. Reinherz, and G. Wagner. 1999. Structure, specificity and CDR mobility of a class II restricted single-chain T-cell receptor. *Nat. Struct. Biol.* 6:574–581.
21. Willcox, B.E., G.F. Gao, J.R. Wyer, J.E. Ladbury, J.I. Bell, B.K. Jakobsen, and P.A. van der Merwe. 1999. TCR binding to peptide-MHC stabilizes a flexible recognition interface. *Immunity.* 10:357–365.
22. Schodin, B.A., C.J. Schlueter, and D.M. Kranz. 1996. Binding properties and solubility of single-chain T cell receptors expressed in *E. coli*. *Mol. Immunol.* 33:819–829.
23. Staerz, U.D., H.G. Rammensee, J.D. Benedetto, and M.J. Bevan. 1985. Characterization of a murine monoclonal antibody specific for an allotypic determinant on T cell antigen receptor. *J. Immunol.* 134:3994–4000.
24. Kranz, D.M., S. Tonegawa, and H.N. Eisen. 1984. Attachment of an anti-receptor antibody to non-target cells renders them susceptible to lysis by a clone of cytotoxic T lymphocytes. *Proc. Natl. Acad. Sci. USA*. 81:7922–7926.
25. Dal Porto, J., T.E. Johansen, B. Catipovic, D.J. Parfiit, D. Tuveson, U. Gether, S. Kozlowski, D.T. Fearon, and J.P. Schneck. 1993. A soluble divalent class I major histocompatibility complex molecule inhibits alloreactive T cells at nanomolar concentrations. *Proc. Natl. Acad. Sci. USA*. 90:6671–6675.
26. O'Herrin, S.M., M.S. Lebowitz, J.G. Bieler, B.K. al-Ramadi, U. Utz, A.L. Bothwell, and J.P. Schneck. 1997. Analysis of the expression of peptide–major histocompatibility complexes using high affinity soluble divalent T cell receptors. *J. Exp. Med.* 186:1333–1345.
27. Sim, B.C., D. Lo, and N.R.J. Gascoigne. 1998. Preferential expression of TCR Vα regions in CD4/CD8 subsets: class discrimination or co-receptor recognition? *Immunol. Today.* 19:276–282.
28. Sim, B.-C., L. Zerva, M.I. Greene, and N.R.J. Gascoigne. 1996. Control of MHC restriction by TCR Vα CDR1 and CDR2. *Science.* 273:963–966.
29. Itano, A., P. Salmon, D. Kioussis, M. Tolaini, P. Corbella, and E. Robey. 1996. The cytoplasmic domain of CD4 promotes the development of CD4 lineage T cells. *J. Exp. Med.* 183:731–741.
30. Matechak, E.O., N. Killeen, S.M. Hedrick, and B.J. Fowlkes. 1996. MHC class II-specific T cells can develop in the CD8 lineage when CD4 is absent. *Immunity.* 4:337–347.
31. Dyall, R., and J. Nikolic-Zugic. 1999. The final maturation of at least some single-positive $CD4^{hi}$ thymocytes does not require T cell receptor–major histocompatibility complex contact. *J. Exp. Med.* 190:757–764.
32. Messaoudi, I., J. LeMaoult, and J. Nikolic-Zugic. 1999. The mode of ligand recognition by two peptide:MHC class I-specific monoclonal antibodies. *J. Immunol.* 163:3286–3294.
33. Speir, J.A., K.C. Garcia, A. Brunmark, M. Degano, P.A. Peterson, L. Teyton, and I.A. Wilson. 1998. Structural basis of the 2C TCR allorecognition of H-$2L^d$ peptide complexes. *Immunity.* 8:553–562.
34. Blackman, M., J. Kappler, and P. Marrack. 1990. The role of the T cell receptor in positive and negative selection of developing T cells. *Science.* 248:1335–1341.
35. Saito, T., J.L. Sussman, J.D. Ashwell, and R.N. Germain. 1989. Marked differences in the efficiency of expression of distinct alpha beta T cell receptor heterodimers. *J. Immunol.* 143:3379–3384.
36. Ignatowicz, L., W. Rees, R. Pacholczyk, H. Ignatowicz, E. Kushnir, J. Kappler, and P. Marrack. 1997. T cells can be activated by peptides that are unrelated in sequence to their selecting peptide. *Immunity.* 7:179–186.
37. Bevan, M.J. 1997. In thymic selection, peptide diversity gives and takes away. *Immunity.* 7:175–178.
38. Sun, R., S.E. Shepherd, S.S. Geier, C.T. Thomson, J.M. Shell, and S.G. Nathenson. 1995. Evidence that the antigen receptors of cytotoxic T lymphocytes interact with a common recognition pattern on the H-$2K^b$ molecule. *Immunity.* 3:573–582.
39. Hornell, T.M., J.C. Solheim, N.B. Myers, W.E. Gillanders, G.K. Balendiran, T.H. Hansen, and J.M. Connolly. 1999. Alloreactive and syngeneic CTL are comparably dependent on interaction with MHC class I alpha-helical residues. *J. Immunol.* 163:3217–3225.
40. Zerrahn, J., W. Held, and D.H. Raulet. 1997. The MHC reactivity of the T cell repertoire prior to positive and negative selection. *Cell.* 88:627–636.
41. Kieke, M.C., E.V. Shusta, E.T. Boder, L. Teyton, K.D. Wittrup, and D.M. Kranz. 1999. Selection of functional T cell receptor mutants from a yeast surface-display library. *Proc. Natl. Acad. Sci. USA.* 96:5651–5656.
42. Shusta, E.V., M.C. Kieke, E. Parke, D.M. Kranz, and K.D. Wittrup. 1999. Yeast polypeptide fusion surface display levels predict thermal stability and soluble secretion efficiency. *J. Mol. Biol.* 292:949–956.
43. Alam, S.M., G.M. Davies, C.M. Lin, T. Zal, W. Nasholds, S.C. Jameson, K.A. Hogquist, N.R. Gascoigne, and P.J. Travers. 1999. Qualitative and quantitative differences in T cell receptor binding of agonist and antagonist ligands. *Immunity.* 10:227–237.
44. Schlueter, C.J., T.C. Manning, B.A. Schodin, and D.M. Kranz. 1996. A residue in the center of peptide QL9 affects binding to both L^d and the T cell receptor. *J. Immunol.* 157: 4478–4485.
45. Eisen, H.N., Y. Sykulev, and T.J. Tsomides. 1996. Antigen-specific T-cell receptors and their reactions with complexes formed by peptides with major histocompatibility complex (MHC) proteins. *Adv. Protein Chem.* 49:1–56.
46. Foote, J., and C. Milstein. 1994. Conformational isomerism and the diversity of antibodies. *Proc. Natl. Acad. Sci. USA.* 91: 10370–10374.
47. Wedemayer, G.J., P.A. Patten, L.H. Wang, P.G. Schultz, and R.C. Stevens. 1997. Structural insights into the evolution of an antibody combining site. *Science.* 276:1665–1669.
48. Boniface, J.J., Z. Reich, D.S. Lyons, and M.M. Davis. 1999. Thermodynamics of T cell receptor binding to peptide-MHC: evidence for a general mechanism of molecular scanning. *Proc. Natl. Acad. Sci. USA.* 96:11446–11451.
49. Daniel, C., S. Horvath, and P.M. Allen. 1998. A basis for alloreactivity: MHC helical residues broaden peptide recognition by the TCR. *Immunity.* 8:543–552.
50. Daniel, C., S. Horvath, and P.M. Allen. 1998. A basis for alloreactivity: MHC helical residues broaden peptide recognition by the TCR. *Immunity.* 8:543–552.